ELSEVIER

Since January 2020 Elsevier has created a COVID-19 resource centre with free information in English and Mandarin on the novel coronavirus COVID-19. The COVID-19 resource centre is hosted on Elsevier Connect, the company's public news and information website.

Elsevier hereby grants permission to make all its COVID-19-related research that is available on the COVID-19 resource centre - including this research content - immediately available in PubMed Central and other publicly funded repositories, such as the WHO COVID database with rights for unrestricted research re-use and analyses in any form or by any means with acknowledgement of the original source. These permissions are granted for free by Elsevier for as long as the COVID-19 resource centre remains active.

ELSEVIER

A novel cell-based binding assay system reconstituting interaction between SARS-CoV S protein and its cellular receptor

Chih-Fong Chou*, Shuo Shen, Yee-Joo Tan, Burtram C. Fielding, Timothy H.P. Tan, Jianlin Fu, Qiurong Xu, Seng Gee Lim, Wanjin Hong

Institute of Molecular and Cell Biology, 61 Biopolis Drive, Proteos, Singapore 138673, Singapore

Abstract

Severe acute respiratory syndrome (SARS), a life-threatening disease, is caused by the newly identified virus SARS coronavirus (SARS-CoV). In order to study the spike (S) protein of this highly contagious virus, we established a clonal cell-line, CHO-SG, from the Chinese hamster ovary cells that stably expresses C-terminally EGFP-tagged SARS-CoV S protein (S-EGFP). The ectodomain of the S glycoprotein is localized on the surface of CHO-SG cells with *N*-acetyl-glucosamine-terminated carbohydrate structure. CHO-SG cells associated tightly with Vero E6 cells, a SARS-CoV receptor (ACE2) expressing cell-line, and the interaction remained stable under highly stringent condition (1 M NaCl). This interaction could be blocked by either the serum from a SARS convalescent patient or a goat anti-ACE2 antibody, indicating that the interaction is specific. A binding epitope with lesser degree of glycosylation and native conformation was localized by using rabbit anti-sera raised against five denatured recombinant S protein fragments expressed in *Escherichia coli*. One of the sera obtained from the fragment encompassing amino acids 48-358 significantly blocked the interaction between CHO-SG and Vero E6 cells. The region is useful for studying neutralizing antibodies in future vaccine development. This paper describes an easy and safe cell-based assay suitable for studying the binding between SARS-CoV S protein and its receptor.
© 2004 Elsevier B.V. All rights reserved.

Keywords: SARS-CoV; Ectodomain; CHO; EGFP-tagged; ACE2; Cell-based assay

1. Introduction

Severe acute respiratory syndrome (SARS), a deadly disease, is caused by a human coronavirus named SARS coronavirus (SARS-CoV). This highly infectious virus killed 774 patients out of 8098 probable SARS cases from November 2002 to July 2003 in 26 countries (Lingappa et al., http://www.cdc.gov/ncidod/EID/vol10no2/03-1032.htm) and had a highly disruptive impact on people's lives as well as the economy. SARS-CoV belongs to the genus of Coronavirus in the family of Coronaviridae, a family of positive sense RNA viruses with large envelopes that propagate in the cytoplasm of host cells and usually cause respiratory diseases in humans and animals. The complete genome of SARS-CoV has been sequenced from different isolates (Marra et al., 2003; Ruan et al., 2003) and it has a coronavirus genome organization with some unique features but is still distantly related to group 2 coronaviruses (Snijder et al., 2003). The genome is nearly 30 kb in length and encodes 14 open reading frames (ORFs) (Marra et al., 2003; Ruan et al., 2003) including those known coronavirus proteins, such as replicase 1a and 1b and four structural proteins, spike (S), envelope (E), membrane (M) and nucleocapsid (N). The rest of the ORFs are novel and may encode for proteins with unknown functions. At least two of these proteins have been shown to be expressed during SARS-CoV infection (Tan et al., 2004b; Yu et al., 2004; Fielding et al., 2004). Antibodies against 3a, also termed as U274, were found in the sera of SARS patients (Tan et al., 2004a; Yu et al., 2004).

Aiming to control the SARS epidemic, we first focused our studies on the S protein for the purpose of diagnosis, and also studied the interaction between S protein and its receptor for vaccine development. The S protein, a type I transmembrane glycoprotein, locates mainly on the outer envelope surface of SARS-CoV. Its precursor is predicted to be 1255 amino acids in length. Residues 1–13 comprise the putative signal peptide and the ectodomain is from residues 14 to 1195 (Marra et al., 2003). A highly hydrophobic region from residues 1196 to 1226 is predicted to be the transmembrane domain and the rest (residues 1227–1255) are located in the cytoplasm. The S protein of coronavirus plays an important role in the initiation of the viral infection by mediating the attachment of the virus to the cell surface receptors that subsequently induces membrane fusion between the virus and the host. In some coronaviruses, the S protein (group II mouse hepatitis virus [MHV] and group III infectious bronchitis virus) is cleaved to generate two distinct functional subunits, S1 and S2, by virus-encoded or host-encoded proteases (Ziebuhr et al., 2000). S1 is the N-terminal fragment responsible for the attachment to the target cells; whereas, S2 is required for the fusion (Gallagher and Buchmeier, 2001). The S2 domain of SARS-CoV S protein can be easily identified by sequence alignment with other coronavirus proteins but the S1 domain is not well conserved (Spiga et al., 2003). Although, currently there is no evidence to show that there are cleaved S1 and S2 subunits in SARS-CoV-infected cells, the S1 equivalent domain has been cloned and demonstrated to bind the SARS-CoV receptor, ACE2, of host cells (Li et al., 2003). Furthermore, the binding domain of the S protein has been narrowed down to the N-terminal amino acid residues 270–510 (Babcock et al., 2004), 303–537 (Xiao et al., 2003) and 318–510 (Wong et al., 2004). In addition to its function in viral entry, the S protein was found to be the major target of the host immune response against coronavirus as it induced neutralizing antibody (Taguchi et al., 1995; Kubo et al., 1994).

Chinese hamster ovary (CHO) cells are useful hosts to express mammalian genes and the system has been studied extensively to produce recombinant therapeutic glycoproteins. CHO cells provide the advantages not only because they can be easily maintained and genetically manipulated, but also because they produce proteins with glycans similar to those native glycoproteins found in humans. In order to avoid the high risks involved in handling live SARS-CoV and to understand the S protein of this virus, we established a CHO clone that expressed a significant amount of the recombinant S proteins on the cell surface and demonstrated that it can be used to study the properties of the SARS-CoV S protein. The selection of a high yield clone was facilitated by tagging the S protein with EGFP at the C-terminus (S-EGFP). The green fluorescence was conveniently used to monitor the expression of the protein in living cells and for observing the cell-based binding assay presented in this paper.

2. Materials and methods

2.1. Cell culture, plasmid construction and transfection

Cell-lines CHO-K1 and Vero E6 were purchased from American Type Cell Collection (Manassas, VA, USA) and cultured at $37\,^{\circ}C$ in 5% CO_2 in DMEM containing $1\,g\,l^{-1}$ glucose, $0.1\,mg\,ml^{-1}$ streptomycin and 100 U penicillin and 10% FBS (HyClone, Utah, USA). To maintain constitutive high level S-EGFP expression in CHO-SG, the culture medium was supplemented with $100\,\mu M$ $ZnSO_4$ (Tan and Hong, 1999). SARS-CoV strain SIN2774 (Ruan et al., 2003), an isolate from a SARS patient in Singapore was used in this study. The cDNA for the cloning of S gene has been previously published (Tan et al., 2004a). The vector pEGFP-N1 as a control for the expression of EGFP was purchased from Clontech (Palo Alto, CA, USA).

Primers for constructing S-EGFP from SARS-CoV strain 2774 (21476–25240) are SARSF (5′-GCCTCGAGGCCAC-CATGTTTATTTTCTTATTATTTCTTACTC-3′) and SAR-SR (5′-GCCCCGGGATGTGTAATGTAATTTGACACCC-3′), the S gene without the stop codon was PCR amplified and inserted into the XhoI/XmaI sites of pEGFP-N1 for making the fusion gene. The plasmid pEGFP-N1-S-EGFP was further digested with XhoI and NotI and then inserted into the XhoI/NotI sites of pMMTC vector (Tan and Hong, 1999). The PCR cycles comprised a denaturation step at $95\,^{\circ}C$ for 2 min, 30 cycles of $95\,^{\circ}C$ for 30 s, $55\,^{\circ}C$ for 1 min, $72\,^{\circ}C$ for 4 min followed by a final elongation step at $72\,^{\circ}C$ for 5 min. The S-EGFP construct was confirmed by DNA sequencing.

Around 80% confluent CHO cells were transfected with S-EGFP and pEGFP-N1 using DMRIE-C (Gibco/BRL, Gaithesburg, MD, USA; Brenner et al., 2002) according to manufacturer's protocol. In general, $2\,\mu g\,ml^{-1}$ DNA construct was mixed with $16\,\mu g\,ml^{-1}$ DMRIE-C in OptiMEM (Gibco/BRL). To obtain stable transfectants, CHO-SG (S-EGFP transfected) and CHO-G (pEGFP-N1 transfected) cells were trypsinized 24 h after transfection and then selected with $1\,mg\,ml^{-1}$ G418 (Gibco/BRL). The expression of EGFP or S-EGFP in transfected cells was detected by using a Leica DMIL-inverted fluorescence microscope fitted with FITC filter.

2.2. Western blot analysis and WGA affinity chromatography

CHO-SG cells were lysed with lysis buffer (1% NP40 in PBS, containing $1\,\mu g\,ml^{-1}$ apotinin [Sigma, St. Louis, MO, USA], 1 mM PMSF [Sigma] on ice for 1 h), and the lysate was then separated on 8% SDS PAGE and transferred to nitrocellulose Hybond C membrane (Amersham-Pharmacia Biotech, Uppsala, Sweden). Prestained molecular markers were purchased from Bio-Rad (Hercules, CA, USA). The membranes were blocked with 5% non-fat milk in PBST (PBS containing 0.2% Tween-20). Antibodies against either GFP (monoclonal, Clontech) or S (polyclonal antibod-

ies from rabbit; Keng et al. (submitted for publication) and horse; Shen et al. (submitted for publication)) were used as primary antibody; horseradish peroxidase (HRP)-conjugated sheep anti-mouse (Amersham-Pharmacia Biotech), goat anti-rabbit (Pierce, Rockford, USA) or goat anti-horse (Bethyl, TX, USA) were used as secondary antibodies and detection was performed with a chemiluminescence kit (Pierce).

S-EGFP was partially purified by using an agarose bound WGA (wheat germ agglutinin; Vector Laboratories, CA, USA) column at 4 °C. CHO-SG cell lysate was first loaded onto WGA column pre-washed with PBS, then the column was washed again with PBS and subsequently three column volumes of 0.5 M N-acetyl-D-glucosamine (GlcNAc; Sigma) in PBS was used to elute the glycoproteins. S-EGFP was identified by Western blot analysis using rabbit anti-S antibody.

2.3. Immunofluorescence analysis

Non-permeable immunofluorescence staining was used to identify cell surface expression of S-EGFP. CHO-SG cells were dislodged with 0.04% EDTA in PBS, and fixed after incubating with primary (patient's serum sample P6 in Tan et al., 2004a) and secondary (Rhodamine-conjugated anti-human IgG [Sigma]) antibody reactions (both antibodies were diluted at 1:20 in growth medium and incubated on ice for 1 h), and then loaded onto black Teflon memzel slides (Merck, Darmstadt, Germany) and fixed with 4% paraformaldehyde. The samples were viewed with a Zeiss microscope (Carl Zeiss Vision GmbH, Hallbergmoss, Germany).

2.4. CHO-SG and Vero E6 cell binding assay

For all the cell-based binding assays presented in this paper, Vero E6 cells were grown to a confluent layer and the CHO-SG and CHO-G cells dislodged by 0.04% EDTA were used as ligands. CHO-SG and CHO-G cells were resuspended in growth medium and a similar amount of cells were laid over the Vero E6 cell layer at 4 °C for 2 h. After the incubation, the cells were washed once with PBS and then three times with PBS containing NaCl of 100 mM, 200 mM, 300 mM, 400 mM, 500 mM or 1 M.

To determine whether ACE2 mediates CHO-SG and Vero E6 interaction, the Vero E6 cell layer was pre-treated with 10 μg ml^{-1} (Li et al., 2003) of goat anti-ACE2 antibody (R&D Systems, MN, USA) in growth medium at 4 °C for 1 h. Then the antibody containing medium was removed, followed by incubation with CHO-SG cells for two more hours. Cells were washed once with PBS and three times with PBS containing 500 mM NaCl.

To test whether the anti-sera from SARS patients or raised against S protein fragments can block the binding between CHO-SG and Vero E6, dislodged CHO-SG cells were pre-incubated with the anti-serum to be tested at 4 °C for 1 h. Then the cells were washed with growth medium and laid over the Vero E6 cell layer for two hours. Cells were washed once with PBS and then three times with 500 mM NaCl. Five rabbit anti-S sera were obtained from the immunizations with recombinant S fragments, SΔ1 (a.a. residues 48–358), SΔ2 (362–790), SΔ3 (168–461), SΔ9 (798–1055) and SΔ10 (1029–1192), expressed in *Escherichia coli* (Keng et al., submitted for publication) and then SDS PAGE separated antigens were purified from gel slices. One mg each of the purified fragments were mixed with equal volume of complete Freud's adjuvant (Sigma) and used to immunize New Zealand white rabbits. All anti-sera used were undiluted including normal human serum and the controls of pre-immune rabbit sera. Results of the cell-based binding assay were detected by using a Leica DMIL-inverted fluorescence microscope fitted with FITC filter. In order to confirm the blocking effect by rabbit anti-S sera, cell lyastes (Vero E6 and CHO-SG binding cells) were analyzed by Western blot using rabbit anti-S antibody.

3. Results

3.1. The construction and expression of S-EGFP

In order to clone the S portion of S-EGFP, we used the viral strain (SIN2774, accession number AY283798) (Ruan et al., 2003) isolated from a SARS patient in Singapore as template for PCR amplification. The primers for amplifying the full-length S gene without the stop codon were designed according to SIN2774 sequence (nucleotides 21476 to 25240); the amplified PCR fragment was fused with the EGFP gene (Fig. 1A) in pEGFP-N1. An extra octapeptide (TRDPPVAT) from the EGFP vector was generated at the junction, which should have limited effect on the transportation and expression of the fusion protein. For the expression of S-EGFP in CHO cells, the fusion construct was then cloned into pMMTC (Tan and Hong, 1999). The transmembrane and cytoplasmic domains of the S protein were retained in the construct for proper anchoring and orientation of the ectodomain on the surface of CHO cells as well as the intracellular localization of EGFP. The expression of S-EGFP was detected by using fluorescence microscope. A stable clone, CHO-SG (Fig. 1B), expressing a relatively high level of S-EGFP at the cytoplasmic membrane was selected for the study described below.

3.2. Western blot analysis and WGA chromatography

Next, we used Western blot analysis to confirm the correct expression. S-EGFP in the cell lysate of CHO-SG (Fig. 2) was identified by a mouse anti-GFP monoclonal antibody (lane A), and two sera from rabbit (lane B) and horse (lane C) raised against the S protein. All the three antibodies recognized a common band of ~220 kDa. The predicted molecular weight (MW) of SARS-CoV S protein is ~180–200 kDa (Xiao et al., 2003); therefore, the MW of S-EGFP is approx-
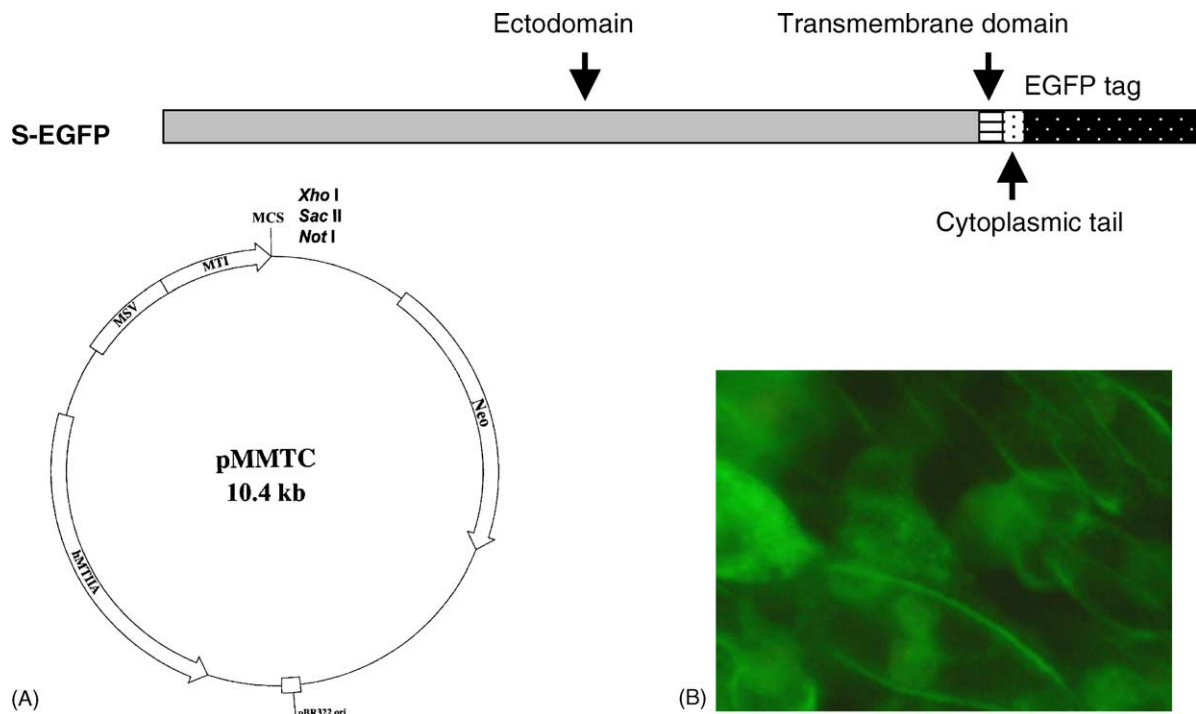
Fig. 1. The construction and expression of S-EGFP. (A) The construct of C-terminal EGFP tagged SARS-CoV S fusion gene (S-EGFP) in the multiple cloning site (MCS) of pMMTC (Tan and Hong, 1999). The expressions were driven by the promoter (MTI) of mouse metallothionein 1 and an enhancer (MSV) from moloney murine sarcoma virus, and the Neo gene was responsible for the selection of G418 resistant cells. (B) The regular culture of CHO-SG, EGFP fluorescence of S-EGFP is localized along the plasma membrane shown as fluorescenced curves.

imately 207–227 kDa with additional 27 kDa from the EGFP tag (Fig. 2). These results concur with the observations from another group (Xiao et al., 2003) that the recombinant S protein was intact in the host cells. Additionally, subcellular fractionation (Chou and Omary, 1994) together with Western blot
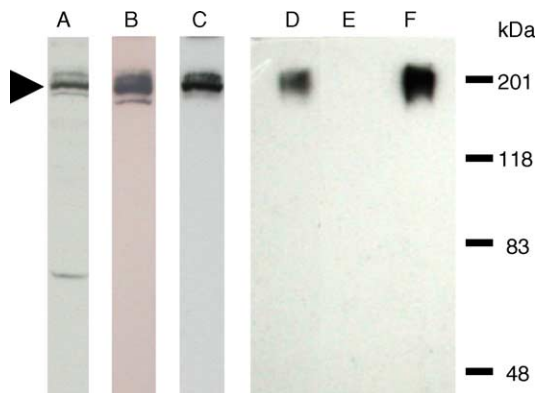

Fig. 2. Western blot analysis to detect S-EGFP from CHO-SG cell lysate and samples prepared by using WGA affinity chromatography. Protein samples were resolved by 8% SDS PAGE and then transferred to a nitrocellulose membrane. Lanes A–C are the identification of S-EGFP in CHO-SG cell lysate. The same membrane was probed with three antibodies separately. Lane A, mouse monoclonal anti-GFP antibody; lane B, rabbit anti-S serum; and lane C, horse anti-S serum. S-EGFP is indicated by the arrowhead. Lanes D–F are the results of WGA chromatography. Lane D, CHO-SG cell lysate; lane E, the flow-through from the WGA column; and lane F, sample eluted from the WGA column. Rabbit anti-S antibody was used for lanes D–F.

analysis showed that S-EGFP was present mainly in the fraction of plasma membrane (data not shown).

The lectin wheat germ agglutinin (WGA) is known for its ability to bind the terminal N-acetyl-glucosamine (GlcNAc) of glycoproteins. In order to determine the carbohydrate characteristics of the glycoprotein S-EGFP, the cell lysate of CHO-SG was passed through a WGA-agarose column. Western blot analysis using rabbit anti-S serum was used to monitor the WGA agarose chromatography. Fig. 2 shows that nearly all S-EGFP was retained on the column (lane F); whereas, it was absent in the flow-through sample (lane E). This result indicates that nearly all S-EGFP molecules are glycosylated with GlcNAc(s) at the end of the oligosaccharide side chains.

3.3. Immunofluorescence analysis using patient's serum

Although Fig. 1B shows that the S-EGFP is localized to the plasma membrane, the result did not provide information about its orientation. Since the ectodomain of the S protein was expected to be outside the cell, non-permeable IFA was applied to confirm the orientation of the fusion protein. A serum sample (P6) from a convalescent SARS patient (Tan et al., 2004a) was used as the primary antibody to stain the CHO-SG cells followed by staining with a Rhodamine-conjugated anti-human IgG (Fig. 3). The normal human serum was used as the negative control. The result indicates that the S portion of S-EGFP was exposed extracellularly of the CHO-SG cells.
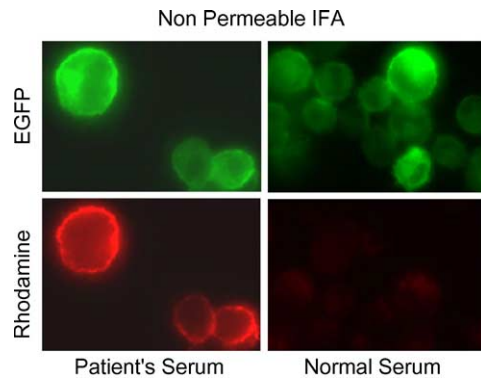
Fig. 3. CHO-SG expresses S-EGFP at cell surface with expected orientation. Non-permeable IFA using the serum (P6 in Tan et al., 2004a) from a recovered SARS patient showed cell surface staining of S-EGFP expressing CHO-SG cells. The control is normal human serum. The green fluorescence seen in the upper panels was from the EGFP tag and the red fluorescence observed in the lower panels was from rhodamine labeled secondary antibody.

3.4. Cell-based binding assay

Since ACE2 on the surface of Vero E 6 cells is responsible for the binding of and the fusion with SARS-CoV (Li et al., 2003), we tested the binding activity between CHO-SG and Vero E6 cells as well as the binding strength between the ligand (SARS-CoV S protein on CHO surface) and the receptor (ACE2 on Vero E6). For the control in the cell-based binding assay, a stable EGFP-expressing CHO clone (CHO-G) was generated by introducing the plasmid pEGFPN1 into CHO cells. Both CHO-G and CHO-SG were tested for binding to Vero E6 cell layers and the results are shown in Fig. 4A. The CHO-G cells resisted the PBS wash but were detached by the solutions containing supplemented NaCl. In contrast, the binding between CHO-SG and Vero E6 could resist up to 1M NaCl. We sought to investigate the binding specificity of this interaction by testing whether the serum from a recovered SARS patient (P8 in Tan et al., 2004a) and a goat anti-ACE2 antibody could block the interaction. To test the blocking effect, either CHO-SG cells were pre-treated with human sera before incubated with Vero E6 cell layers, or Vero E6 cells were pre-treated with anti-ACE2 antibody before interacting with CHO-SG. All panels in Fig. 4B were washed with 500 mM NaCl, the controls for the patient's serum was normal human serum, and for anti-ACE2 was PBS. The results showed that both the patient's serum and the anti-ACE2 antibody could block the binding, suggesting that this binding is specifically mediated by the S protein and ACE2.

Although, the receptor for SARS-CoV has been found, it is still important to localize the epitopes that induce neutralizing antibody against the virus, particularly for the purposes of vaccine development. We attempted to localize the epitopes by expressing 5 recombinant S fragments (Fig. 5A) in *E. coli* and then immunizing rabbits with the purified fragments. To determine which anti-serum may block the binding, CHO-SG cells were pre-treated with the 5 rabbit sera individually

before incubating with Vero E6 cell layers. After the incubation, the cells were washed once with PBS and 3 times with 500 mM NaCl. The anti-SΔ1 serum demonstrated the blocking effect (Fig. 5B and C) indicating that some blocking epitopes are present in SΔ1.

4. Discussion

CHO-SG that constitutively expresses a significant amount of S-EGFP provides a convenient tool to study the recombinant SARS-CoV S protein. Our results showed that the ectodomain of the S protein on the surface of CHO cells mimics the interaction between the virus and Vero E6 cells, presumably through the cellular receptor ACE2. The cell-based binding assay introduced in this paper should facilitate the screening for drugs, peptides or vaccines that block the entry of SARS-CoV, minimizing the use of the highly infectious live virus. The clonal cell-line CHO-SG may be used for large-scale production to supply S-EGFP as a diagnostic marker, and its affinity to WGA is a favorable property to assist the purification of S-EGFP. Although, the expression of S-EGFP on CHO-SG was significant, self-fusion of CHO-SG cells has not been observed in culture, which may be due to the absence or a low level of ACE2 on CHO (ovary) cells (Donoghue et al., 2000). The expressions of recombinant S protein in full-length or fragments had been demonstrated previously (Li et al., 2003; Xiao et al., 2003; Wong et al., 2004) by using human kidney cell-lines 293 or 293T. We also tried two human cell-lines, 293T and Jurkat, to express S-EGFP but stable clones were not established due to the undetectable green fluorescence from G418 resistant colonies.

The SARS convalescent patient's sera (P6 and P8 in Tan et al., 2004a) blocked the interaction between CHO-SG cells and Vero E6, confirming the authenticity of this assay. Serum sample P6 does efficiently identify the extracellular expression of the S ectodomain on the cell surface of CHO-SG by non-permeable IFA (Fig. 3), but with lower potency to block the binding (data not shown in Fig. 4B). Epitopes of SARS-CoV S protein responsible for the binding to ACE2 was first demonstrated to be in the S1 region (Li et al., 2003) and then narrowed down to the amino acid residues 270–510 (Babcock et al., 2004), 303–537 (Xiao et al., 2003) and 318–510 (Wong et al., 2004). The binding and fusion interactions were performed by using expressed soluble S fragments and the cellular receptor. We used the cell-based binding assay to test the blocking effect for five rabbit anti-S sera raised against five recombinant S fragments and three of these fragments, SΔ1, SΔ2 and SΔ3 (Fig. 5A) covered the a.a. residues from 48 to 790, which overlapped with the predicted S1 domain (Li et al., 2003) or the S-ACE2 binding region. However, we were only able to identify a significant blocking effect (Fig. 5B and C) from anti-SΔ1 (a.a. 48–358) rabbit serum. In order to rule out non-specific effects from undiluted serum, pre-immune rabbit sera were used as the controls for the binding assay and no blocking effect was ob-
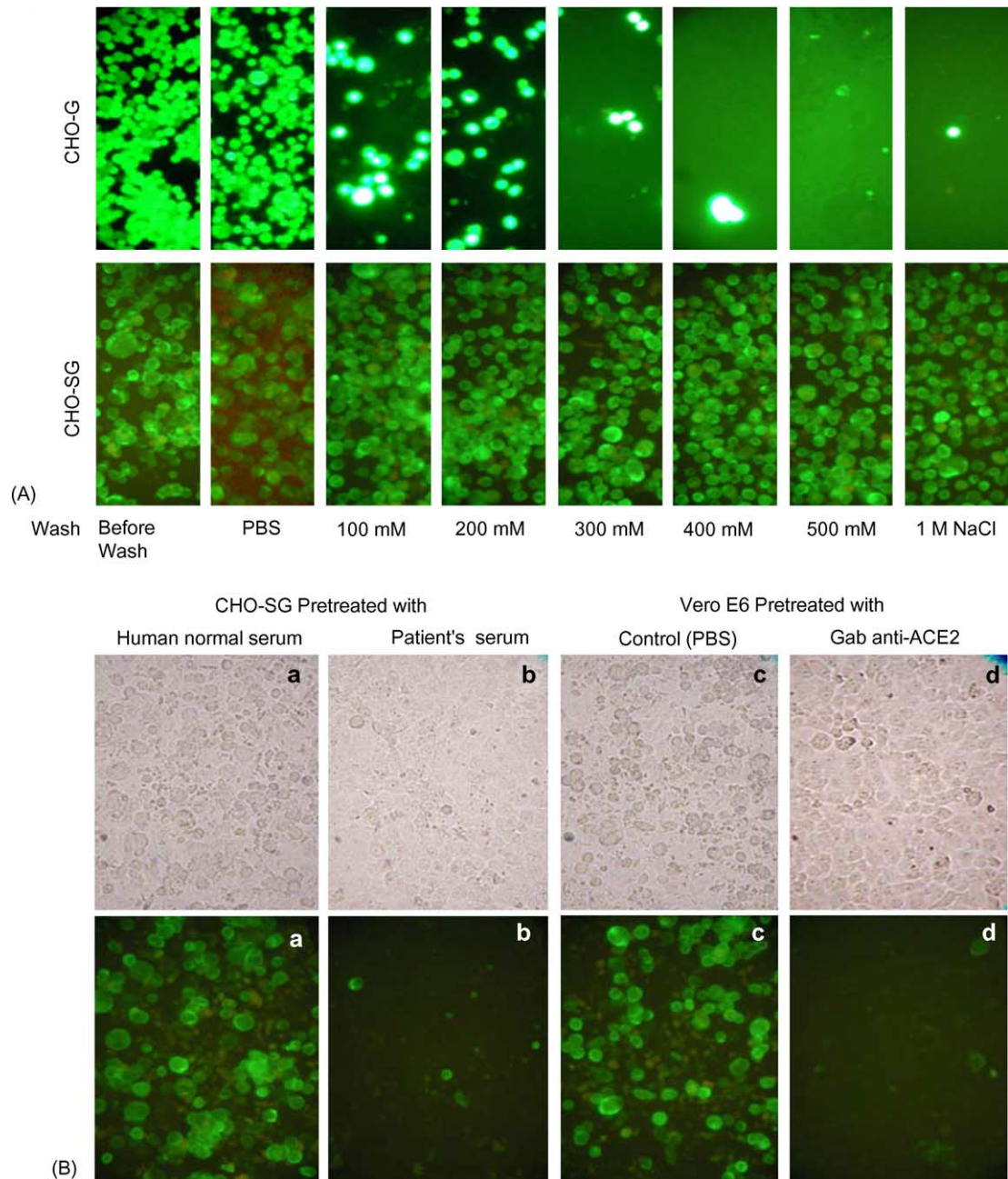
Fig. 4. CHO-SG and Vero E6 binding assay. In all panels, Vero E6 cells were first cultured to a confluent layer. (A) EDTA dislodged CHO-G (upper panels) and CHO-SG (lower panels) were incubated with the Vero E6 cell layers in the cold room for 2 h. Cells were washed once with PBS and followed by three washes with PBS containing different amounts of NaCl as indicated at the bottom of the figure. (B) The photos shown in the upper panels were taken under tungsten lamp and these in the lower panels were taken under green fluorescence. CHO-SG cells were pre-treated with either human normal serum (a) or SARS recovered patient's serum (P8 in Tan et al., 2004a) (b) before being added to the Vero E6 cell layer. The cells were washed with 500 mM NaCl after the incubation with Vero E6 cells. Vero E6 cultures were pre-treated with goat anti-ACE2 antibody (d) or the PBS control (c) and then incubated with the CHO-SG cells followed by 500 mM NaCl washes.

served. The rabbit sera produced against fragment S∆3 (a.a. 168–461) and S∆10 (1029–1192) also presented some minor blocking effects (Fig. 5B and C). Rabbit serum anti-S∆2 (a.a. 362–790) could not block the binding (or anti-S∆3 with less significant effect) may be due to the antigenicities for those modules requiring higher extent of glycosylation or the native conformation. However, although the region of S∆1

contains nine predicted *N*-glycosylation sites, the rabbit antiserum raised against the denatured fragment produced from *E. coli* was still able to block the binding. This indicates that there is a non-glycosylated and linear epitope within S∆1 that is important for S-ACE2 binding. Although the rabbit anti-S serum against S∆3 could not block the binding effectively, it was routinely used in a dilution of 1:2000 as primary anti-
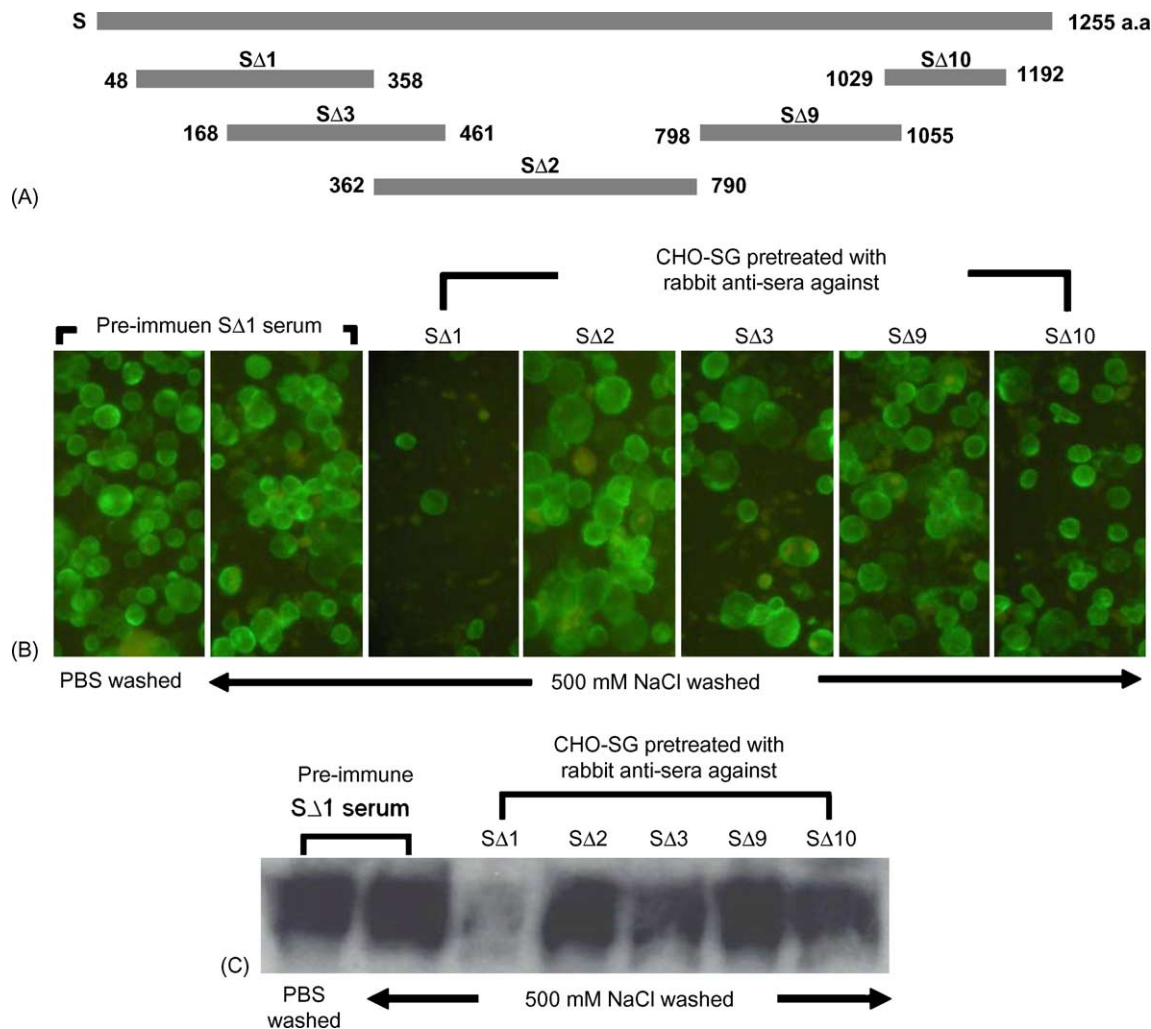
Fig. 5. Identification of the receptor-binding region of SARS-CoV S gene. (A) Five fragments of SARS-CoV S protein were expressed in *E. coli*. Rabbits were immunized with these five recombinant S protein fragments. The rabbit anti-sera were tested for blocking CHO-SG and Vero E6 cell interaction. (B) The CHO-SG cells were first treated with pre-immune serum or one of five rabbit anti-sera described in (A), and then added to the Vero E6 cell layer. After incubation, the cells were washed with 500 mM NaCl. The rabbit serum from SΔ1 had the most significant blocking effect. (C) Western blot analysis using rabbit anti-S antibody to show the amount of S-EGFP in (B) samples.

body for Western blot analysis (Fig. 2). All sera from either humans or rabbits used in the binding assay were neat; however, diluted sera (1:10) were tested and revealed insignificant blocking effect. Our results identified a receptor binding domain of the S protein required lesser extent of glycosylation and native conformation.

The blockage of CHO-SG cells to Vero E6 cells by anti-ACE2 antibody was nearly complete (Fig. 4B), indicating that ACE2 is the main receptor on the surface of Vero E6 cells responsible for the binding. However, we cannot exclude the possibilities of other receptors involved in the binding, such as the one closely associated with ACE2, which may also be blocked by an anti-ACE2 antibody. In patients with SARS, atypical pneumonia and diarrhea were common symptoms caused by SARS-CoV, correspondingly the mRNA levels of ACE2 were comparably high in gastrointestinal system and lung (Harmer et al., 2002) and the higher ACE2 protein levels

have been demonstrated in the epithelia of the lung and small intestine (Hamming et al., 2004). Two human lung cell-lines (MRC5 and A549) and a human colon cell-line (HT29) were tested for developing the binding assay but results were unexpected due to non-specific binding between CHO-SG and these cells. Other human cell line of lung or digestive tissues will be examined in the future.

Acknowledgements

ported by the Agency for Science and Technology (A*STAR) of Singapore.

References

Babcock, G.J., Esshaki, D.J., Thomas Jr., W.D., Ambrosino, D.M., 2004. Amino acids 270 to 510 of the severe acute respiratory syndrome coronavirus spike protein are required for interaction with receptor. J. Virol. 78 (9), 4552–45560.

Brenner, S., Venkatesh, B., Yap, W.H., Chou, C.F., Tay, A., Ponniah, S., Wang, Y., Tan, Y.H., 2002. Conserved regulation of the lymphocyte-specific expression of *lck* in the Fugu and mammals. Proc. Natl. Acad. Sci. U.S.A. 99, 2936–2941.

Chou, C.F., Omary, M.B., 1994. Mitotic arrest with anti-microtubule agents or okadaic acid is associated with increased glycoprotein terminal GlcNAc's. J. Cell Sci. 107, 1833–1843.

Donoghue, M., Hsieh, F., Baronas, E., Godbout, K., Gosselin, M., Stagliano, N., Donovan, M., Woolf, B., Robison, K., Jeyaseelan, R., Breitbart, R.E., Acton, S., 2000. A novel angiotensin-converting enzyme-related carboxypeptidase (ACE2) converts angiotensin I to angiotensin 1–9. Circ. Res. 87, E1–E9.

Fielding, B.C., Tan, Y.J., Shuo, S., Tan, T.H., Ooi, E.E., Lim, S.G., Hong, W.J., Goh, P.Y., 2004. Characterization of a unique group-specific protein (u122) of the severe acute respiratory syndrome coronavirus. J. Virol. 78, 7311–7318.

Gallagher, T.M., Buchmeier, M.J., 2001. Coronavirus spike proteins in viral entry pathogenesis. Virology 279, 371–374.

Hamming, I., Timens, W., Bulthuis, M., Lely, A., Navis, G., Van Goor, H., 2004. Tissuedistribution of ACE2 protein, the functional receptor for SARS coronavirus. A first step in understanding SARS pathogenesis. J. Pathol. 203, 631–637.

Harmer, D., Gilbert, M., Borman, R., Clark, K.L., 2002. Quantitative mRNA expression profiling of ACE2, a novel homologue of angiotensin converting enzyme. FEBS Lett. 532, 107–110.

Keng, C.T., Zhang A.H., Shen, S., Tan Y.J., Lip, K.M., Fielding B.C., Tan T.H.P., Chou C.F., Wang S.F., Fu J.L., Lim, S.G., Hong, W.J. Amino acids 1055 to 1192 in the S2 domain of SARS coronavirus S protein induces neutralizing antibodies: implications for the development of vaccine and anti-viral agent, submitted for publication.

Kubo, H., Yamada, Y.K., Taguchi, F., 1994. Localization of neutralizing epitopes and the receptor-binding site within the amino-terminal 330 amino acids of the murine coronavirus spike protein. J. Virol. 68, 5403–5410.

Li, W., Moore, M.J., Vasilieva, N., Sui, J., Wong, S.K., Berne, M.A., Somasundaran, M., Sullivan, J.L., Luzuriaga, K., Greenough, T.C., Choe, H., Farzan, M., 2003. Angiotensin-converting enzyme 2 is a functional receptor for the SARS coronavirus. Nature 426, 450–454.

Lingappa J.R., McDonald, L.C., Simone, P., Parashar, U.D., 2004. Wresting SARS from uncertainty. Emerg. Infect. Dis., 10. http://www.cdc.gov/ncidod/EID/vol10no2/03-1032.htm.

Marra, M.A., Jones, S.J., Astell, C.R., Holt, R.A., Brooks-Wilson, A., Butterfield, Y.S., Khattra, J., Asano, J.K., Barber, S.A., Chan, S.Y., Cloutier, A., Coughlin, S.M., Areeman, D., Girn, N., Griffith, O.L., Leach, S.R., Mayo, M., AcDonald, H., Montgomery, S.B., Pandoh, P.K., Petrescu, A.S., Robertson, A.G., Schein, J.E., Siddiqui, A.,
Smailus, D.E., Stott, J.M., Yang, G.S., Plummer, F., Andonov, A., Artsob, H., Bastien, N., Bernard, K., Booth, T.F., Bowness, D., Czub, M., Drebot, M., Fernando, L., Flick, R., Garbutt, M., Gray, M., Grolla, A., Jones, S., Feldmann, H., Meyers, A., Kabani, A., Li, Y., Normand, S., Stroher, U., Tipples, G.A., Tyler, S., Vogrig, R., Ward, D., Watson, B., Brunham, R.C., Krajden, M., Petric, M., Skowronski, D.M., Upton, C., Roper, R.L., 2003. The genome sequence of the SARS-associated coronavirus. Science 300, 1399–1404.

Ruan, Y.J., Wei, C.L., Ee, A.L., Vega, V.B., Thoreau, H., Su, S.T., Chia, J.M., Ng, P., Chiu, K.P., Lim, L., Zhang, T., Peng, C.K., Lin, E.O., Lee, N.M., Yee, S.L., Ng, L.F., Chee, R.E., Stanton, L.W., Long, P.M., Liu, E.T., 2003. Comparative full-length genome sequence analysis of 14 SARS coronavirus isolates and common mutations associated with putative origins of infection. Lancet 361, 1779–1785.

Shen, S., Tan, Y.J., Goh, P.Y. Keng, C.T., Lip, K.M., Zhang, A., Loh, C.B., Wang, S., Fielding, B.C., Tan, T.H., Chou, C.F., Hwang, L.A., Fang, Z.H., Yang, X.M., Lin, W., Shen, X.L., Ooi, E.E., Liu, D.X., Lan, T-P. H., Fu, J.L., Lim, S.G., Hong., W.J., Expression, processing and maturation of the spike (S) protein of severe acute respiratory syndrome coronavirus (CoV), submitted for publication.

Snijder, E.J., Bredenbeek, P.J., Dobbe, J.C., Thiel, V., Ziebuhr, J., Poon, L.L., Guan, Y., Rozanov, M., Spaan, W.J., Gorbalenya, A.E., 2003. Unique and conserved features of genome and proteome of SARS-coronavirus, an early split-off from the coronavirus group 2 lineage. J. Mol. Biol. 331, 991–1004.

Spiga, O., Bernini, A., Ciutti, A., Chiellini, S., Menciassi, N., Finetti, F., Causarono, V., Anselmi, F., Prischi, F., Niccolai, N., 2003. Molecular modelling of S1 and S2 subunits of SARS coronavirus spike glycoprotein. Biochem. Biophys. Res. Commun. 310, 78–83.

Taguchi, F., Kubo, H., Suzuki, H., Yamada, Y.K., 1995. Localization of neutralizing epitopes and receptor-binding site in murine coronavirus spike protein. Adv. Exp. Med. Biol. 380, 359–365.

Tan, Y.H., Hong, W.J. 1999. Gene expression in mammalian cells, UK Patent GB2314332B.

Tan, Y.J., Goh, P.Y., Fielding, B., Shen, S., Chou, C.F., Fu, J.L., Leong, H.N., Leo, Y.S., Ooi, E.E., Ling, A.E., Lim, S.G., Hong, W.J., 2004a. Profile of antibody responses against SARS-Coronavirus recombinant proteins and their potential use as dianostic markers. Clin. Diag. Lab. Immunol. 11, 362–371.

Tan, Y.J., Teng, E., Shen, S., Tan, T.H., Goh, P.Y., Fielding, B.C., Ooi, E.E., Tan, H.C., Lim, S.G., Hong, W.J., 2004b. A novel severe acute respiratory syndrome coronavirus protein, U274, is transported to the cell surface and undergoes endocytosis. J. Virol. 78, 6723–6734.

Wong, S.K., Li, W., Moore, M.J., Choe, H., Farzan, M., 2004. A 193-amino-acid fragment of the SARS coronavirus S protein efficiently binds angiotensin-converting enzyme 2. J. Biol. Chem. 279, 3197–3201.

Xiao, X., Chakraborti, S., Dimitrov, A.S., Gramatikoff, K., Dimitrov, D.S., 2003. The SARS-CoV S glycoprotein: expression and functional characterization. Biochem. Biophys. Res. Commun. 312, 1159–1164.

Yu, C.J., Chen, Y.C., Hsiao, C.H., Kuo, T.C., Chang, S.C., Lu, C.Y., Wei, W.C., Lee, C.H., Huang, L.M., Chang, M.F., Ho, H.N., Lee, F.J., 2004. Identification of a novel protein 3a from severe acute respiratory syndrome coronavirus. FEBS Lett. 565, 111–116.

Ziebuhr, J., Snijder, E.J., Gorbalenya, A.E., 2000. Virus-encoded proteinases and proteolytic processing in the Nidovirales. J. Gen. Virol. 81, 853–879.